

Synthesis, Characterization, and Reactivity of [Ru(bpy)(CH₃CN)₃(NO₂)]PF₆, a Synthron for [Ru(bpy)(L₃)NO₂] Complexes

Daniel A. Freedman,* Seth Kruger, Christina Roosa, and Chandra Wymer

Department of Chemistry, State University of New York at New Paltz, New Paltz, New York 12561

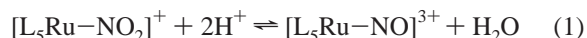
Received June 9, 2006

We report a high yield, two-step synthesis of *fac*-[Ru(bpy)(CH₃CN)₃(NO₂)]PF₆ from the known complex [(*p*-cym)Ru(bpy)Cl]PF₆ (*p*-cym = *η*⁶-*p*-cymene). [(*p*-cym)Ru(bpy)NO₂]PF₆ is prepared by reacting [(*p*-cymene)Ru(bpy)Cl]PF₆ with AgNO₃/KNO₂ or AgNO₂. The ¹⁵NNO₂ analogue is prepared using K¹⁵NO₂. Displacement of *p*-cymene from [(*p*-cym)Ru(bpy)NO₂]PF₆ by acetonitrile gives [Ru(bpy)(CH₃CN)₃(NO₂)]PF₆. The new complexes [(*p*-cym)Ru(bpy)NO₂]PF₆ and *fac*-[Ru(bpy)(CH₃CN)₃(NO₂)]PF₆ have been fully characterized by ¹H and ¹⁵N NMR, IR, elemental analysis, and single-crystal structure determination. Reaction of [Ru(bpy)(CH₃CN)₃(NO₂)]PF₆ with the appropriate ligands gives the new complexes [Ru(bpy)(Tp)NO₂] (Tp = HB(pz)₃⁻, pz = 1-pyrazolyl), [Ru(bpy)(Tpm)NO₂]PF₆ (Tpm = HC(pz)₃), and the previously prepared [Ru(bpy)(trpy)NO₂]PF₆ (trpy = 2,2',6',2''-terpyridine). Reaction of the nitro complexes with HPF₆ gives the new nitrosyl complexes [Ru(bpy)TpNO][PF₆]₂ and [Ru(bpy)(Tpm)NO][PF₆]₃. All complexes were prepared with ¹⁵N-labeled nitro or nitrosyl groups. The nitro and nitrosyl complexes were characterized by ¹H and ¹⁵N NMR and IR spectroscopy, elemental analysis, cyclic voltammetry, and single-crystal structure determination for [Ru(bpy)TpNO][PF₆]₂. For the nitro complexes, a linear correlation is observed between the nitro ¹⁵N NMR chemical shift and 1/*ν*_{asym}, where *ν*_{asym} is the asymmetric stretching frequency of the nitro group.

Introduction

There has been considerable interest in the chemistry of ruthenium–nitro (NO₂) and –nitrosyl (NO) complexes. Ruthenium–nitrosyl complexes have been the subject of numerous studies relating to their potential applications in nitrosyl-releasing or scavenging complexes, as well as their fundamentally interesting redox, electronic, and structural properties.^{1–28} Interest in ruthenium–nitro complexes is

partially due to their use as synthetic precursors for nitrosyl complexes through the equilibrium shown in reaction 1^{29,30}



Separate interest in ruthenium–nitro complexes stems from

* To whom correspondence should be addressed. E-mail: freedmad@newpaltz.edu.

- (1) Sarkar, S.; Sarkar, B.; Chanda, N.; Kar, S.; Mobin, S. M.; Fiedler, J.; Kaim, W.; Lahiri, G. K. *Inorg. Chem.* **2005**, *44*, 6092.
- (2) Roncaroli, F.; Olabe, J. A. *Inorg. Chem.* **2005**, *44*, 4719.
- (3) Czap, A.; Heinemann, F. W.; van Eldik, R. *Inorg. Chem.* **2004**, *43*, 7832.
- (4) Chanda, N.; Mobin, S. M.; Puranik, V. G.; Datta, A.; Niemeyer, M.; Lahiri, G. *Inorg. Chem.* **2004**, *43*, 1056.
- (5) Patra, A. K.; Mascharak, P. K. *Inorg. Chem.* **2003**, *42*, 7363.
- (6) Sauaia, M. G.; da Silva, R. S. *Transition Met. Chem.* **2003**, *28*, 254.
- (7) Roncaroli, F.; Baraldo, L. M.; Slep, L. D.; Olabe, J. A. *Inorg. Chem.* **2002**, *41*, 1930.
- (8) Roncaroli, F.; Ruggiero, M. E.; Franco, D. W.; Estiu, G. L.; Olabe, J. A. *Inorg. Chem.* **2002**, *41*, 5760.
- (9) Works, C. F.; Jocher, C. J.; Bart, G. D.; Bu, X.; Ford, P. C. *Inorg. Chem.* **2002**, *41*, 3278.
- (10) Hadadzadeh, H.; DeRosa, M. C.; Yap, G. P. A.; Rezvani, A. R.; Crutchley, R. J. *Inorg. Chem.* **2002**, *41*, 6521.
- (11) Togniolo, V.; da Silva, R. S.; Tedesco, A. C. *Inorg. Chim. Acta* **2001**, *316*, 7.

- (12) Mondal, B.; Paul, H.; Puranik, V. G.; Lahiri, G. K. *J. Chem. Soc., Dalton Trans.* **2001**, 481.
- (13) Lopes, L. G. F.; Wieraszko, A.; El-Sharif, Y.; Clarke, M. J. *Inorg. Chim. Acta* **2001**, *312*, 15.
- (14) Works, C. F.; Ford, P. C. *J. Am. Chem. Soc.* **2000**, *122*, 7592.
- (15) McGarvey, B. R.; Ferro, A. A.; Tfouni, E.; Bezerra, C. W. B.; Bagatin, I.; Franco, D. W. *Inorg. Chem.* **2000**, *39*, 3577.
- (16) Lang, D. R.; Davis, J. A.; Lopes, L. G. F.; Ferro, A. A.; Vasconcellos, L. C. G.; Franco, D. W.; Tfouni, E.; Wieraszko, A.; Clarke, M. J. *Inorg. Chem.* **2000**, *39*, 2294.
- (17) Bezerra, C. W. B.; da Silva, S. C.; Gambardella, M. T. P.; Santos, R. H. A.; Plicas, L. M. A.; Tfouni, E.; Franco, D. W. *Inorg. Chem.* **1999**, *38*, 5660.
- (18) Chen, Ya.; Lin, F.; Shephard, R. E. *Inorg. Chem.* **1999**, *38*, 973.
- (19) Gomes, M. G.; Davanzo, C. U.; Silva, S.; Lopes, L. G. F.; Santos, P. S.; Franco, D. W. *J. Chem. Soc., Dalton Trans.* **1998**, 601.
- (20) Borges, S. S.; Davanzo, C. U.; Castellano, E. E.; Z-Schpector, J.; Silva, S. C.; Franco, D. W. *Inorg. Chem.* **1998**, *37*, 2670.
- (21) Lorkovic, I. M.; Miranda, K. M.; Lee, B.; Bernhad, S.; Schooner, J. R.; Ford, P. C. *J. Am. Chem. Soc.* **1998**, *120*, 11674.
- (22) Ford, P. C.; Bourassa, J.; Miranda, K.; Lee, B.; Lorkovic, I.; Boggs, S.; Kudo, S.; Laverman, L. *Coord. Chem. Rev.* **1998**, *171*, 185.
- (23) Fricker, S. P.; Slade, E.; Powell, N. A.; Vaughan, O. J.; Henderson, G. R.; Murrer, B. A.; Megson, I. L.; Bisland, S. K.; Flitney, F. W. *Br. J. Pharmacol.* **1997**, *122*, 1441.

studies of their ligand substitution and linkage isomerization reactions as well as their potential as oxo-atom transfer agents.^{31–46}

Our interest is in developing more general synthetic methods for preparing ruthenium–nitro compounds. Although a significant number of different complexes have been studied, the synthetic methodology is generally restricted to a few starting materials. For instance, a significant number of $[\text{Ru}(\text{L}_2)(\text{trpy})\text{NO}_2]$ complexes have been prepared starting from $[\text{Ru}(\text{trpy})\text{Cl}_3]$, but we could find only one report of ruthenium–nitro complexes with a tridentate ligand other than trpy,⁴⁷ even though nitro and nitrosyl complexes of fac-coordinating tridentate ligands such as $[\text{HB}(\text{pz})_3]^-$ are potentially interesting. Although ruthenium–nitro complexes with these ligands could probably be prepared by standard methods, we thought it should be possible to develop a more general approach by preparing a synthetic intermediate with a nitro group and several labile ligands to which a wide variety of ligands could be added. This would be a significant departure from the universally used route in which the nitro group is added in the final step of the synthesis and would make it possible to prepare a variety of new complexes in a single step from a common synthon.

We are also interested in making it more economical to prepare ^{15}N -labeled nitro and nitrosyl complexes. ^{15}N labeling dramatically simplifies the assignment of the complex IR

spectra of these compounds and makes it possible to collect ^{15}N NMR data, a useful characterization tool for nitro and nitrosyl complexes.^{31,18} Preparing ^{15}N -labeled ruthenium–nitro complexes using standard methods is costly because the nitro group is invariably added by refluxing a suitable aqua or chloro complex with a 10–20-fold excess of nitrite ion.

It has been shown that ruthenium complexes containing acetonitrile ligands, $[\text{CpRu}(\text{CH}_3\text{CN})_3]\text{PF}_6$ ⁴⁸ ($\text{Cp} = \eta^5\text{-cyclopentadienyl}$) and $[\text{Ru}(\text{bpy})(\text{CH}_3\text{CN})_3\text{Cl}]\text{Cl}$ ⁴⁹ for example, are useful synthons. Both of these complexes were prepared by the photochemical displacement of an η^6 -coordinated benzene ligand in acetonitrile solution. We thought a similar strategy could be employed here if a suitable ruthenium–arene complex containing a nitro ligand could be prepared. Recent work suggested that $[\text{BzRu}(\text{bpy})\text{NO}_2]^+$ ($\text{Bz} = \eta^6\text{-C}_6\text{H}_6$) is present as an intermediate in the reaction of $[\text{BzRu}(\text{bpy})\text{Cl}]^+$ with excess nitrite ion to give $[\text{Ru}(\text{bpy})(\text{NO}_2)_4]^{2-}$.⁵⁰ Although it was reported that $[\text{BzRu}(\text{bpy})\text{NO}_2]^+$ could not be isolated, presumably due to the lability of the benzene ring, it seems likely that a stable analogous complex could be prepared using an alkylated arene ligand as alkyl substituents stabilize metal–arene bonds. Herein we report the preparation of $[(p\text{-cym})\text{Ru}(\text{bpy})\text{NO}_2]^+$ from which $[\text{Ru}(\text{bpy})(\text{CH}_3\text{CN})_3\text{NO}_2]\text{PF}_6$ is synthesized by thermal displacement of the *p*-cymene ring. We also demonstrate that $[\text{Ru}(\text{bpy})(\text{CH}_3\text{CN})_3\text{NO}_2]\text{PF}_6$ is a useful synthon for $[\text{Ru}(\text{bpy})(\text{L}_3)\text{NO}_2]$ complexes.

General Experimental Considerations

KNO_2 , K^{15}NO_2 , 2,2'-bipyridine, 2,2',6',2''-terpyridine, and RuCl_3 were purchased from Aldrich. $\text{KHB}(\text{pz})_3 \cdot \text{H}_2\text{O}$ and $\text{HC}(\text{pz})_3$ were purchased from Strem. AgNO_2 was prepared by mixing equal molar amounts of AgNO_3 and KNO_2 in an aqueous solution to give a precipitate of AgNO_2 that was isolated by filtration, washed with ice water, and dried in vacuo. All synthetic procedures were carried out under an inert Ar or N_2 atmosphere unless otherwise noted. Elemental analyses were performed by MHW Laboratories. ^1H NMR and ^{15}N NMR spectra were recorded on a JEOL 300 MHz Eclipse+ spectrometer. ^1H NMR chemical shifts are relative to $(\text{CH}_3)_4\text{Si}$. ^{15}N chemical shifts are externally referenced to neat $\text{CD}_3\text{-NO}_2$. UV–vis spectra were recorded on an Ocean Optics Chem 2000 spectrometer. IR spectra were recorded on a Perkin-Elmer 1600 FTIR equipped with a Pike Technologies MIRacle ATR sampling accessory or a Nicolet 4700 IR spectrometer. Cyclic voltammetry data were collected on a BAS 100B electrochemical analyzer as previously described.⁵¹ Potentials are referenced to aqueous Ag/AgCl (1 M KCl) and are not corrected for the junction potential.

Compound Synthesis

Procedure A for $[(p\text{-cym})\text{Ru}(\text{bpy})\text{NO}_2]\text{PF}_6$. $[(p\text{-cym})\text{Ru}(\text{bpy})\text{Cl}]\text{PF}_6$ (2.814 g, 4.92 mmol) and AgNO_3 (0.836 g, 4.92 mmol) were added to 30 mL of methanol. The mixture was stirred for 5 min, and KNO_2 (0.502 g, 5.90 mmol) was added. After stirring for 18 h, an excess of NH_4PF_6 was added and the mixture was cooled

- (24) Davies, N. A.; Wilson, M. T.; Slade, E.; Fricker, S. P.; Murrer, B. A.; Powell, N. A.; Henderson, G. R. *Chem. Commun.* **1997**, 47.
 (25) Fricker, S. P. *Platinum Met. Rev.* **1995**, 39, 150.
 (26) Deb, A. K.; Paul, P. C.; Goswami, S. *J. Chem. Soc., Dalton Trans.* **1988**, 2051.
 (27) Pipes, D. W.; Meyer, T. J. *Inorg. Chem.* **1984**, 23, 2466.
 (28) Callahan, R. W.; Meyer, T. J. *Inorg. Chem.* **1977**, 16, 574.
 (29) Godwin, J. B.; Meyer, T. J. *Inorg. Chem.* **1971**, 10, 471.
 (30) Godwin, J. B.; Meyer, T. J. *Inorg. Chem.* **1971**, 10, 2150.
 (31) Freedman, D. A.; Janzen, D. E.; Vreeland, J.; Tully, H. M.; Mann, K. R. *Inorg. Chem.* **2002**, 41, 3820.
 (32) Ooyama, D.; Nagao, H.; Ito, K.; Nagao, N.; Howell, F. S.; Mukaida, M. *Bull. Chem. Soc. Jpn.* **1997**, 70, 2141.
 (33) Leising, R. A.; Kubow, S. A.; Szczepura, L. F.; Takeuchi, K. *J. Inorg. Chim. Acta.* **1996**, 245, 167.
 (34) Dovletoglou, A.; Adeyemi, S. A.; Meyer, T. J. *Inorg. Chem.* **1996**, 35, 4120.
 (35) Ooyama, D.; Nagao, H.; Nagao, N.; Howell, F.; Mukaida, M. *Chem. Lett.* **1996**, 759.
 (36) Ooyama, D.; Nagao, N.; Nagao, H.; Miura, Y.; Hasegawa, A.; Ando, K.; Howell, F. S.; Mukaida, M.; Tanaka, K. *Inorg. Chem.* **1995**, 34, 6024.
 (37) Nagao, N.; Ooyama, D.; Oomura, K.; Miura, Y.; Howell, F. S.; Mukaida, M. *Inorg. Chim. Acta* **1994**, 225, 111.
 (38) Rhodes, M. R.; Barley, M. H.; Meyer, T. J. *Inorg. Chem.* **1991**, 30, 629.
 (39) Leising, R. A.; Takeuchi, K. *J. Am. Chem. Soc.* **1988**, 110, 4079.
 (40) Murphy, W. R.; Takeuchi, K.; Barley, M. H.; Meyer, T. J. *Inorg. Chem.* **1986**, 25, 1041.
 (41) Nagao, H.; Howell, F. S.; Mukaida, M.; Kakihana, M. *J. Chem. Soc., Chem. Commun.* **1987**, 1618.
 (42) Abruna, H. D.; Walsh, J. L.; Meyer, T. J.; Murray, R. W. *Inorg. Chem.* **1981**, 20, 1481.
 (43) Abruna, H. D.; Walsh, J. L.; Meyer, T. J.; Murray, R. W. *J. Am. Chem. Soc.* **1980**, 102, 3272.
 (44) Keene, F. R.; Salmon, D. J.; Walsh, J. L.; Abruna, H. D.; Meyer, T. J. *Inorg. Chem.* **1980**, 19, 1896.
 (45) Keene, F. R.; Salmon, D. J.; Meyer, T. J. *J. Am. Chem. Soc.* **1977**, 99, 4821.
 (46) Keene, F. R.; Salmon, D. J.; Meyer, T. J. *J. Am. Chem. Soc.* **1977**, 99, 2384.
 (47) Bessel, C. A.; See, R. F.; Jameson, D. L.; Churchill, M. R.; Takeuchi, K. *J. Chem. Soc., Dalton Trans.* **1993**, 1563.

- (48) Gill, T. P.; Mann, K. R. *Organometallics* **1982**, 1, 484.
 (49) Freedman, D. A.; Evju, J. K.; Pomije, M. K.; Mann, K. R. *Inorg. Chem.* **2001**, 40, 5711.
 (50) Freedman, D. A.; Janzen, D. E.; Mann, K. R. *Inorg. Chem.* **2001**, 40, 6009.
 (51) Graf, D. D.; Mann, K. R. *Inorg. Chem.* **1997**, 36, 150.

in an ice bath. The precipitate, which consisted of AgCl(s) and the desired product, was isolated by filtration and then stirred in 30 mL of acetone for 10 min. The insoluble AgCl(s) was filtered off on a short column of diatomaceous earth. The volume of acetone was reduced to ca. 10 mL by rotary evaporation. Addition of diethyl ether precipitated the product, which was filtered off and washed with diethyl ether to give 2.67 g (93.1% yield) of a light yellow powder. Anal. Calcd for [(*p*-cym)Ru(bpy)NO₂]PF₆: C, 41.23; H, 3.81; N, 7.22. Found: C, 40.80; H, 3.79; N, 7.43. ¹H NMR (300 MHz, d⁶-acetone, δ): 9.688 (ddd, bpy-H^{6,6'}, *J*₁ = 5.78 Hz, *J*₂ = 1.38 Hz, *J*₃ = 0.55 Hz); 8.615 (d, bpy-H^{3,3'}, *J*₁ = 7.71 Hz); 8.369 (td, bpy-H^{4,4'}, *J*₁ = 7.71 Hz, *J*₂ = 1.38 Hz); 7.874 (ddd, bpy-H^{5,5'}, *J*₁ = 7.43 Hz, *J*₂ = 5.78 Hz, *J*₃ = 1.38 Hz); 6.331 and 6.123 (d, CH₃C₆H₄CH(CH₃)₂, *J* = 6.33 Hz); 2.750 (hept, CH₃C₆H₄CH(CH₃)₂, *J* = 6.88 Hz); 2.267 (s, CH₃C₆H₄CH(CH₃)₂); 1.062 (d, CH₃C₆H₄CH(CH₃)₂, *J* = 6.88 Hz).

Procedure B for [(*p*-cym)Ru(bpy)NO₂]PF₆. [(*p*-cym)Ru(bpy)Cl]PF₆ (1.014 g, 1.77 mmol) and AgNO₂ (0.333 g, 2.17 mmol) were added to 30 mL of methanol. The mixture was stirred for 18 h, an excess of NH₄PF₆ was added, and the mixture was cooled in an ice bath. The precipitate that formed was isolated by filtration and then stirred in 30 mL of acetone for 10 min. The insoluble AgCl(s) was filtered off on a short column of diatomaceous earth. The volume of acetone was reduced to ca. 10 mL by rotary evaporation. Addition of diethyl ether precipitated the product, which was filtered off and washed with diethyl ether to give 0.792 g (78.0% yield) of a light yellow powder. The ¹H NMR of the product was identical to that prepared by procedure A.

[Ru(bpy)(CH₃CN)₃NO₂]PF₆. [(*p*-cym)Ru(bpy)NO₂]PF₆ (1.00 g, 1.72 mmol) was added to an oven-dried, 50 mL, three-necked round-bottom flask equipped with a nitrogen inlet, stir bar, reflux condenser, and rubber septum. Freshly distilled acetonitrile (10 mL) and methylene chloride (20 mL) were added by syringe. The solution was purged with nitrogen and then refluxed for 20 h, after which it was cooled in an ice bath, producing a bright orange precipitate that was filtered off and washed with diethyl ether. Addition of a small amount of diethyl ether to the filtrate produced a second crop of orange powder. The overall yield was 0.746 g (76.0%). Anal. Calcd for [Ru(bpy)(CH₃CN)₃NO₂]PF₆: C, 33.63; H, 3.00; N, 14.71. Found: C, 33.80; H, 3.28; N, 14.71. ¹H NMR (300 MHz, CD₃CN, δ): 9.083 (d, bpy-H^{6,6'}, *J* = 5.64 Hz); 8.335 (d, bpy-H^{3,3'}, *J* = 7.98 Hz); 8.067 (apparent td, bpy-H^{4,4'}, *J*₁ = 7.71 Hz, *J*₂ = 1.38 Hz); 7.584 (ddd bpy-H^{5,5'}, *J*₁ = 7.43 Hz, *J*₂ = 5.78 Hz, *J*₃ = 1.38 Hz); 2.600 (s, CH₃CN, *cis* to NO₂); 2.071 (s, CH₃-CN, *trans* to NO₂).

[Ru(bpy)TpNO₂]. [Ru(bpy)(CH₃CN)₃NO₂]PF₆ (0.200 g, 0.35 mmol) and KHB(pz)₃·H₂O (0.088 g, 0.35 mmol) were added to an oven-dried, 25 mL, three-necked round-bottom flask equipped with a nitrogen inlet, stir bar, reflux condenser, and rubber septum. Freshly distilled acetone (10 mL) was added via syringe. The solution was purged with nitrogen and then refluxed for 1 h, after which the solution was cooled and the acetone removed by rotary evaporation. The residue was taken up in 10 mL of methylene chloride, and the mixture was filtered through a short column of diatomaceous earth. Addition of diethyl ether produced a precipitate that was filtered off and washed with diethyl ether. The product was isolated as a brownish-maroon powder (0.133 g, 73.6%). Anal. Calcd for Ru(bpy){HB(pz)₃}NO₂: C, 44.19; H, 3.52; N, 24.40. Found: C, 44.40; H, 4.14; N, 24.16. ¹H NMR (300 MHz, CD₂Cl₂, δ) 8.713 (d, bpy-H^{6,6'}, *J* = 5.50 Hz); 8.278 (d, bpy-H^{3,3'}, *J* = 7.98 Hz); 8.037 (d, pz-H^{3,3'}, *J* = 1.65 Hz); 7.866 (td, bpy-H^{4,4'}, *J*₁ = 7.98 Hz, *J*₂ = 1.38 Hz); 7.830 (d, pz-H^{5,5'}, *J* = 2.20 Hz); 7.715 (d, pz-H⁵, *J* = 2.20 Hz); 7.298 (ddd, bpy-H^{5,5'}, *J*₁ = 7.43 Hz, *J*₂ =

5.78 Hz, *J*₃ = 1.38 Hz); 6.376 (apparent t, pz-H^{4,4'}, *J* = 2.20 Hz); 6.058 (d, pz-H³, *J* = 1.93 Hz); 5.907 (apparent t, pz-H⁴, *J* = 2.20 Hz). Note that pz_t refers to the pyrazol ring *trans* to the nitro group.

[Ru(bpy)(Tpm)NO₂]PF₆. [Ru(CH₃CN)₃(bpy)NO₂]PF₆ (174 mg, 0.300 mmol) and tris(1-pyrazolyl)methane (66.3 mg, 0.300 mmol) were added to an oven-dried, 25 mL, three-necked round-bottom flask equipped with a nitrogen inlet, stir bar, reflux condenser, and rubber septum. Freshly distilled acetone (10 mL) was added via syringe. The solution was refluxed for ~1 h. The solution was initially cloudy yellow, orange after 10 min, and dark red after 20 min. The solution was cooled to room temperature, and the product was precipitated by adding diethyl ether and cooling to -15 °C. The precipitate was filtered off and washed with two 5 mL portions each of dichloromethane and diethyl ether to give a light orange powder (0.118 g, 88.7%). Anal. Calcd for [Ru(bpy){HC(pz)₃}NO₂]PF₆: C, 36.26; H, 2.74; N, 19.03. Found: C, 35.99; H, 2.66; N, 18.97. ¹H NMR (300 MHz, d⁶-acetone, δ): 9.842 (s, HC(Pz)₃); 8.914 (d, bpy-H^{6,6'}, *J* = 5.50 Hz); 8.698 (d, bpy-H^{3,3'}, *J* = 7.69 Hz); 8.653 (d, pz-H^{3,3'}, *J* = 2.19 Hz); 8.638 (dd, pz-H^{5,5'}, *J*₁ = 2.88 Hz, *J*₂ = 0.82 Hz); 8.571 (dd, pz_t-H⁵, *J*₁ = 2.88 Hz, *J*₂ = 0.55 Hz); 8.191 (td, bpy-H^{4,4'}, *J*₁ = 7.89 Hz, *J*₂ = 1.09 Hz); 7.665 (ddd, bpy-H^{5,5'}, *J*₁ = 7.69 Hz, *J*₂ = 5.76 Hz, *J*₃ = 1.37 Hz); 7.004 (dd, pz_t-H³, *J*₁ = 2.19 Hz, *J*₂ = 0.55 Hz); 6.785 (dd, pz-H^{4,4'}, *J*₁ = 2.74 Hz, *J*₂ = 2.19 Hz); 6.410 (dd, pz_t-H⁴, *J*₁ = 2.89 Hz, *J*₂ = 2.19 Hz). Note that pz_t refers to the pyrazol ring *trans* to the nitro group.

[Ru(bpy)(trpy)NO₂]PF₆. [Ru(bpy)(CH₃CN)₃NO₂]PF₆ (116.9 mg, 0.205 mmol) and 2,2':6',2''-terpyridine (49.3 mg, 0.211 mmol) were added to an oven-dried, 25 mL, three-necked round-bottom flask equipped with a nitrogen inlet, stir bar, reflux condenser, and rubber septum. Freshly distilled acetone (10 mL) was added via syringe. The solution was refluxed for ~1 h, changing color from orange to brown after ~10 min. The solution was cooled to room temperature, and the product was precipitated by adding diethyl ether and cooling to -15 °C. The precipitate was filtered on a glass frit and washed with diethyl ether to give a dark brown powder (0.123 g, 87.9%). ¹H NMR (300 MHz, d⁶-acetone, δ): 10.011 (ddd, bpy-H⁶, *J*₁ = 5.64 Hz, *J*₂ = 1.38 Hz, *J*₃ = 0.83 Hz); 8.871 (d, bpy-H³, *J* = 7.69 Hz); 8.742 (d, trpy-H^{3,5'}, *J* = 7.98 Hz); 8.65 (obscured, bpy-H³); 8.614 (ddd, trpy-H^{3,3'}, *J*₁ = 8.19 Hz, *J*₂ = 1.38 Hz, *J*₃ = 0.83 Hz); 8.395 (apparent td, bpy-H⁴, *J*₁ = 7.85 Hz, *J*₂ = 1.65 Hz); 8.315 (t, trpy-H⁴, *J* = 7.98 Hz); 8.09 (obscured, bpy-H⁵); 8.056 (apparent td, trpy-H^{5,5'}, *J*₁ = 7.98 Hz, *J*₂ = 1.65 Hz); 7.924 (ddd, bpy-H⁴, *J*₁ = 7.84 Hz, *J*₂ = 7.71 Hz, *J*₃ = 1.38 Hz); 7.898 (ddd, trpy-H^{6,6'}, *J*₁ = 5.50 Hz, *J*₂ = 1.65 Hz, *J*₃ = 0.83 Hz); 7.634 (ddd, bpy-H⁶, *J*₁ = 5.64 Hz, *J*₂ = 1.38 Hz, *J*₃ = 0.83 Hz); 7.434 (ddd, trpy-H^{4,4'}, *J*₁ = 7.71 Hz, *J*₂ = 5.50 Hz, *J*₃ = 1.38 Hz); 7.217 (ddd, bpy-H⁵, *J*₁ = 7.57 Hz, *J*₂ = 5.64 Hz, *J*₃ = 1.38 Hz).

[Ru(bpy)TpNO₂]PF₆·2. [Ru(bpy)TpNO₂] (0.050 g, 0.097 mmol) was dissolved in 5 mL of freshly distilled methylene chloride to give a maroon solution. Two drops of 60% HPF₆ was added. The solution was stirred for 1 h, during which time a dark precipitate formed. The precipitate was isolated by filtration and dissolved in acetonitrile, and the solution was passed through a short column of diatomaceous earth. Addition of diethyl ether and cooling at -15 °C overnight yielded 38 mg (50%) of a mixture of reddish-orange needles and orange powder. Anal. Calcd for [Ru(bpy)TpNO₂]PF₆·2H₃CN: C, 30.34; H, 2.55; N, 16.85. Found: C, 30.52; H, 2.45; N, 16.79. ¹H NMR (300 MHz, d⁶-acetone, δ) 9.164 (dd, bpy-H^{3,3'}, *J*₁ = 8.26 Hz, *J*₂ = 1.10 Hz); 8.950 (dd, bpy-H^{6,6'}, *J*₁ = 5.78 Hz, *J*₂ = 1.10 Hz); 8.794 (d, pz-H^{3,3'}, *J* = 2.20 Hz); 8.782 (apparent td, bpy-H^{4,4'}, *J*₁ = 7.98 Hz, *J*₂ = 1.38 Hz); 8.437 (d, pz-H^{5,5'}, *J* = 2.48 Hz); 7.307 (d, pz_t-H⁵, *J* = 2.48 Hz); 8.112 (ddd, bpy-H^{5,5'}, *J*₁ = 7.71 Hz, *J*₂ = 5.78 Hz, *J*₃ = 1.38 Hz); 7.146 (d, pz_t-H³, *J* =

2.48 Hz); 6.860 (apparent t, pz-H^{4,4'}, *J* = 2.48 Hz); 6.355 (t, pz_i-H⁴, *J* = 2.48 Hz). Note that pz_i refers to the pyrazol ring trans to the nitrosyl group.

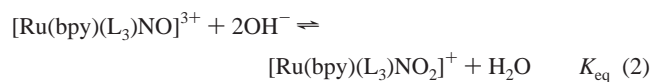
[Ru(bpy)(Tpm)NO][PF₆]₃. [Ru(bpy)(Tpm)NO₂][PF₆] (140.1 mg, 0.213 mmol) was placed in a 25 mL round-bottom flask and dissolved in 10 mL of freshly distilled dichloromethane to give an orange solution. Hexafluorophosphoric acid (60%) was added (0.19 mL, 2.1 mmol) dropwise with stirring. The solution was stirred for 15 min, during which time a yellow precipitate formed on the bottom of the flask. The supernatant was decanted, leaving a yellow precipitate that was washed with several portions of diethyl ether to give 188 mg (94.5%) of product. Anal. Calcd for [Ru(bpy)NO-(HC(pz)₃)]PF₆·2O: C, 25.17; H, 2.12; N, 13.21. Found: C, 25.38; H, 2.04; N, 12.82. ¹H NMR (300 MHz, d⁶-acetone, δ): 10.628 (s, HC(Pz)₃); 9.310 (d, pz-H^{3,3'}, *J* = 2.75 Hz); 9.193 (dd, bpy-H^{3,3'}, *J*₁ = 8.11 Hz, *J*₂ = 0.96); 9.136 (dd, bpy-H^{6,6'}, *J*₁ = 5.92 Hz, *J*₂ = 1.37); 9.042 (d, pz-H^{5,5'}, *J* = 3.02); 8.927 (d, pz_i-H⁵, *J* = 2.47 Hz); 8.829 (apparent td, bpy-H^{4,4'}, *J*₁ = 7.97 Hz, *J*₂ = 1.38 Hz); 8.150 (ddd, bpy-H^{5,5'}, *J*₁ = 7.71 Hz, *J*₂ = 5.78 Hz, *J*₃ = 1.38 Hz); 7.735 (d, pz_i-H³, *J* = 2.75); 7.158 (apparent t, pz-H^{4,4'}, *J* = 2.75); 6.704 (apparent t, pz_i-H⁴, *J* = 2.75). Note that pz_i refers to the pyrazol ring trans to the nitrosyl group.

[Ru(bpy)(Tpm)NO₂]Cl. [Ru(bpy)(Tpm)NO₂][PF₆] (83.0 mg, 0.125 mmol) was placed in a 25 mL round-bottom flask and dissolved in 10 mL of freshly distilled acetonitrile. Tetrabutylammonium chloride (60.0 mg, 0.216 mmol) was added to the solution. After stirring for 10 min, a reddish-orange precipitate formed. The supernatant was decanted, and the precipitate was washed with diethyl ether. The product was dried in vacuo to give 63.2 mg (91.6%) of product. ¹H NMR (300 MHz, D₂O, δ): 9.585 (s, HC-(Pz)₃); 8.639 (d, bpy-H^{3,3'}, *J* = 8.26 Hz); 8.554 (d, bpy-H^{6,6'}, *J* = 5.23 Hz); 8.454 (d, pz-H^{5,5'}, *J* = 3.03 Hz); 8.312 (d, pz_i-H⁵, *J* = 3.03 Hz); 8.148 (apparent td, bpy-H^{4,4'}, *J*₁ = 7.84 Hz, *J*₂ = 1.10 Hz); 8.088 (d, pz-H^{3,3'}, *J* = 2.20 Hz); 7.464 (ddd, bpy-H⁵, *J*₁ = 7.26 Hz, *J*₂ = 5.76 Hz, *J*₃ = 0.90 Hz); 6.70–6.74 (m, pz-H^{4,4'} and pz_i-H³); 6.269 (apparent t, pz_i-H⁴, *J* = 2.48 Hz). Note that pz_i refers to the pyrazol ring trans to the nitro group.

[Ru(bpy)(trpy)NO₂][Cl]. [Ru(bpy)(trpy)NO₂][PF₆] (0.116 g, 0.170 mmol) and tetrabutylammonium chloride (0.704 g, 2.53 mmol) were treated the same as above to give 96.1 mg (99%) of a brown powder. ¹H NMR (300 MHz, D₂O, δ): 9.480 (d, bpy-H⁶, *J* = 5.23 Hz); 8.615 (d, bpy-H³, *J* = 7.98 Hz); 8.498 (d, trpy-H^{3,5'}, *J* = 7.98 Hz); 8.35–8.38 (m, trpy-H^{3,3''} and bpy-H³); 8.264 (apparent t, bpy-H⁴, *J* = 7.68 Hz); 8.217 (t, trpy-H⁴, *J* = 8.25 Hz); 7.89–7.96 (m, trpy-H^{5,5'}, bpy-H⁵); 7.785 (apparent t, bpy-H⁴, *J* = 7.43 Hz); 7.740 (d, trpy-H^{6,6'}, *J* = 5.50 Hz); 7.362 (d, bpy-H⁶, *J* = 5.50 Hz); 7.28 (apparent t, trpy-H^{4,4''}, *J* = 6.33 Hz); 7.023 (apparent t, bpy-H⁵, *J* = 6.33 Hz).

¹⁵NO₂- and ¹⁵NO-Labeled Compounds. All of the compounds above were prepared with the nitro or nitrosyl group labeled with ¹⁵N. This was accomplished by using K¹⁵NO₂ (procedure A) in the preparation of [(*p*-cym)Ru(bpy)NO₂][PF₆] in place of KNO₂ to give [(*p*-cym)Ru(bpy)¹⁵NO₂][PF₆]. Subsequent reactions were then carried out in the same manner as described above. The ¹⁵N-labeled complexes were characterized by ¹H NMR, ¹⁵N NMR, and IR spectroscopy (Table 3).

Equilibrium Studies. The equilibrium constant for reaction 2 was determined for L₃ = Tpm, trpy. Buffers (0.010 M) were prepared from pH 2.0 to 5.3 by the addition of NaOH (6 and 1 M)



or HClO₄ (6 M) to potassium hydrogen phthalate solutions. Buffer solutions were 1.0 M in NaCl to maintain constant ionic strength. At least five solutions at different pH's were prepared with a [Ru-(bpy)(L₃)NO₂]Cl (L₃ = trpy, Tpm) complex concentration of ca. 1 × 10⁻⁴ M by diluting a stock solution of the appropriate ruthenium complex with a particular buffer. The solutions were thermostated at 25.0 (±0.1) °C, and the absorbance spectra were monitored over a period of time until absorbance values were unchanged between two consecutive measurements. This was approximately 2 days for [Ru(bpy)(trpy)NO₂]⁺ and 3 h for [Ru(bpy)(Tpm)NO₂]⁺. For the latter complex, further non-isosbestic changes in the UV-vis spectrum occurred after ca. 1 day, indicating that slow decomposition of [Ru(bpy)(Tpm)NO₂]⁺ and [Ru(bpy)(Tpm)NO]³⁺ had occurred.

The equilibrium constant for reaction 2 was determined using the Scatchard equation, which can be derived for this system (eq 3). In eq 3, Δ*A* is the difference between the absorbance of a mixture

$$\Delta A = -K_{\text{eq}}(\Delta A)[\text{OH}^-]^2 + (\Delta \epsilon)[\text{Ru}]_0 \quad (3)$$

containing both nitro and nitrosyl species and the absorbance of pure [Ru(bpy)(L₃)NO₂]⁺, Δ*ε* is the difference between the molar extinction coefficients of the nitrosyl and nitro forms, and [Ru]₀ is the total concentration of all ruthenium species. The plot of Δ*A* versus Δ*A*[OH⁻]² has a slope equal to -*K*_{eq}.

X-ray Structure Determination. X-ray diffraction data were collected on a Bruker SMART APEX 2 CCD platform diffractometer (Mo Kα (λ = 0.710 73 Å)) at 115 K. Suitable crystals were mounted in a nylon loop with Paratone-N cryoprotectant oil. The structures were solved using direct methods and standard difference map techniques and were refined by full-matrix least-squares procedures on *F*² with SHELXTL (Version 6.14).⁵² Hydrogen atoms were included in the calculated position. Crystal data and refinement details are presented in Table 1. Selected bond lengths and angles are given in Table 2.

[(*p*-cym)Ru(bpy)NO₂]PF₆. Suitable X-ray quality single crystals of [(*p*-cym)Ru(bpy)NO₂]PF₆ were grown from an acetone/diethyl ether mixture at -15 °C. An ORTEP diagram of the cation of [(*p*-cym)Ru(bpy)NO₂]⁺ is shown in Figure 1.

[Ru(bpy)(CH₃CN)₃NO₂]PF₆. Suitable X-ray quality single crystals of [Ru(bpy)(CH₃CN)₃NO₂]⁺PF₆ were grown by slow diffusion of diethyl ether into an acetonitrile solution of the complex. An ORTEP diagram of the cation of [Ru(bpy)(CH₃CN)₃NO₂]⁺PF₆ is shown in Figure 2. A view of a portion of the unit cell is shown in Figure 3.

[Ru(bpy)(Tp)NO][PF₆]₂. Suitable X-ray quality single crystals of [Ru(bpy)(Tp)NO][PF₆]₂ were grown by slow diffusion of diethyl ether into an acetonitrile solution of the complex. Both of the hexafluorophosphate anions are disordered. The atoms of these anions were included in the refinement using the program SQUEEZE in the PLATON suite of programs.⁵³ SQUEEZE found two 867 Å³ voids at (0, 0, 0.499) and (0, 0.500, 0.588) in the unit cell, each containing electron density totaling 500 electrons. This compared well to the 447 electrons expected for the eight hexafluorophosphate anions that should be contained in each void. The elemental analysis of this compound indicated that acetonitrile may also be present in the crystal, which may account for the excess electron density. An ORTEP diagram of the cation of [Ru(bpy)(Tp)NO][PF₆]₂ is shown in Figure 4.

(52) Sheldrick, G. M. *SHELXTL: An Integrated System for Solving, Refining, and Displaying Crystal Structures from Diffraction Data*; University of Göttingen: Göttingen, Germany, 1981.

(53) Van der Sluis, P.; Spek, A. L. *Acta Crystallogr., Sect. A* **1990**, *46*, 194.

Table 1. Crystal Data, Data Collection, and Refinement Parameters for [(*p*-cym)Ru(bpy)NO₂]PF₆ (1), *fac*-[Ru(bpy)(CH₃CN)₃NO₂]PF (2), and Ru(bpy)TpNO₂ (3)

compound formula	1	2	3
compound formula	C ₂₀ H ₂₂ F ₆ N ₃ O ₂ -PRu	C ₁₆ H ₁₇ F ₆ N ₆ O ₂ PRu	C ₁₉ H ₂₃ BF ₁₂ N ₉ -OP ₃ Ru
habit, color	plate, yellow	plate, yellow	needle, red
size, mm	0.33 × 0.20 × 0.10	0.30 × 0.18 × 0.05	0.20 × 0.08 × 0.04
lattice type	orthorhombic	monoclinic	monoclinic
space group	<i>Pbca</i>	<i>P2₁/n</i>	<i>C2/c</i>
<i>a</i> , Å	12.3474(2)	8.8820(2)	28.472(3)
<i>b</i> , Å	13.8298(2)	15.7248(3)	12.681(1)
<i>c</i> , Å	25.2511(4)	15.4441(3)	15.403(2)
β , deg		90.620(1)	98.334(1)
<i>V</i> , Å ³	4311.9(1)	2156.92(8)	5503(1)
<i>Z</i>	8	4	8
fw, g mol ⁻¹	582.45	571.40	795.28
<i>D_c</i> , mg m ⁻³	1.794	1.760	1.908
μ , mm ⁻¹	0.877	0.878	0.803
<i>F</i> (000)	2336	1136	3120
θ range, deg	1.61–28.31	1.85–30.64	1.76–25.56
index ranges	–16 ≤ <i>h</i> ≤ 16 –18 ≤ <i>k</i> ≤ 18 –33 ≤ <i>l</i> ≤ 33	–12 ≤ <i>h</i> ≤ 12 –22 ≤ <i>k</i> ≤ 22 –22 ≤ <i>l</i> ≤ 22	–34 ≤ <i>h</i> ≤ 34 –15 ≤ <i>k</i> ≤ 15 –18 ≤ <i>l</i> ≤ 18
reflections collected	72061	39977	25898
unique reflections	5372 (<i>R</i> _{int} = 0.0606)	6519 (<i>R</i> _{int} = 0.0421)	5159 (<i>R</i> _{int} = 0.0683)
weighting factors, ^a <i>a</i> , <i>b</i>	0.0273, 0.3406	0.0403, 2.1501	0.0337, 0.000
max, min transmission	0.9174, 0.7607	0.9574, 0.7786	0.9857, 0.8558
data/restraints/parameters	5372/0/302	6519/0/292	5159/0/280
<i>R</i> ₁ , <i>wR</i> ₂ (<i>I</i> > 2σ(<i>I</i>) =)	0.0262, 0.0547	0.0342, 0.0781	0.0401, 0.0761
<i>R</i> ₁ , <i>wR</i> ₂ (all data)	0.0378, 0.0580	0.0485, 0.0847	0.0596, 0.0802
goodness of fit (on <i>F</i> ²)	1.033	1.016	1.016
largest diff peak, hole, e Å ⁻³	0.423, –0.444	0.755, –0.847	0.449, –0.549

$$^a w = [\sigma^2(F_o^2) + (aP)^2 + (bP)]^{-1}, \text{ where } P = (F_o^2 + 2F_c^2)/3.$$

Results

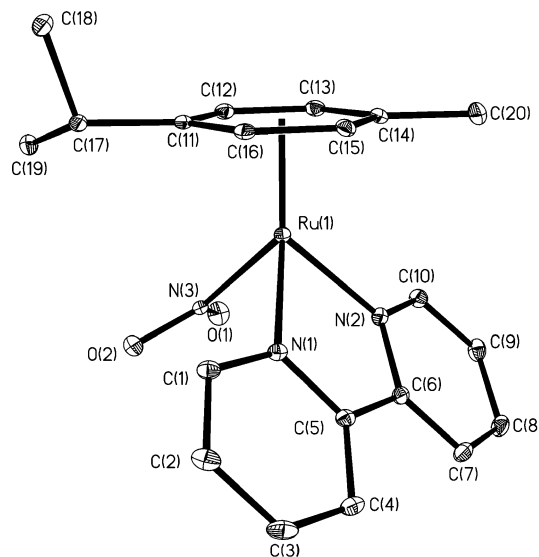
Preparation of [Ru(bpy)(CH₃CN)₃NO₂]PF₆. Scheme 1 shows the synthetic route for the preparation of [Ru(bpy)-NO₂(CH₃CN)₃]PF₆. [(*p*-cym)Ru(bpy)Cl]PF₆ was prepared from [(*p*-cym)RuCl₂] as described previously.⁵⁴ Reaction of this complex in methanol with AgNO₃ and KNO₂ (procedure A) or AgNO₂ (procedure B) at room temperature gives [(*p*-cym)Ru(bpy)NO₂]PF₆ as a pale yellow powder in good yield. This complex is indefinitely stable when stored at –15 °C but will decompose slowly at room temperature. It was characterized by ¹H and ¹⁵N NMR and IR spectroscopy, elemental analysis, and single-crystal structure determination. The ¹⁵NO₂ analogue was prepared by using K¹⁵-NO₂ in place of KNO₂ in procedure A. Reaction of [(*p*-cym)Ru(bpy)NO₂]PF₆ in a 2:1 mixture of refluxing CH₂-Cl₂/CH₃CN over 20 h gave clean conversion to [Ru(bpy)-(CH₃CN)₃NO₂]PF₆. Reaction in neat acetonitrile also resulted in loss of the *p*-cymene ring but caused further decomposition to unknown products. The ¹H NMR spectrum of [Ru(bpy)-(CH₃CN)₃NO₂]PF₆ shows two acetonitrile methyl resonances in a 2:1 ratio and four bipyridine proton signals, consistent with the *fac* geometry shown in Scheme 1. The ¹H NMR data, taken in CD₃CN, clearly show that the acetonitrile ligands are labile. In the initial spectrum, the integral of the signal for the methyl protons on the acetonitrile trans to the nitro group showed that one-third of these acetonitriles had exchanged with solvent and the resonance for the acetonitriles

(54) Janzen, D. E.; Wang, X.; Carr, P. W.; Mann, K. R. *Inorg. Chim. Acta* **2004**, *357*, 3317.

Table 2. Selected Bond Lengths (Å) and Angles (deg)^a for [(*p*-cym)Ru(bpy)NO₂]PF₆ (1), *fac*-[Ru(bpy)(CH₃CN)₃NO₂]PF (2), and Ru(bpy)TpNO₂ (3)

	1	2	3
Ru–N(1)	2.075(2)	2.047(2)	2.087(3)
Ru–N(2)	2.084(2)	2.041(2)	2.072(3)
Ru–N(3)	2.073(2)	2.014(2)	1.753(3)
Ru–N(4)	<i>b</i>	2.046(2)	2.077(3)
Ru–N(5)	<i>b</i>	2.076(2)	2.053(3)
Ru–N(6)	<i>b</i>	2.045(2)	2.074(2)
Ru–cent ^c	1.710	<i>b</i>	<i>b</i>
N(3)–O(1)	1.218(2)	1.250(2)	1.138(3)
N(3)–O(2)	1.252(2)	1.245(2)	<i>b</i>
N(1)–Ru–N(2)	77.18(6)	79.35(7)	78.7(2)
N(1)–Ru–N(3)	84.34(6)	90.90(7)	95.9(1)
N(1)–Ru–N(4)	<i>b</i>	95.23(7)	97.5(1)
N(1)–Ru–N(5)	<i>b</i>	89.98(7)	88.0(1)
N(1)–Ru–N(6)	<i>b</i>	176.18(7)	173.2(1)
N(2)–Ru–N(3)	84.52(6)	89.99(17)	92.9(1)
N(2)–Ru–N(4)	<i>b</i>	173.56(7)	172.8(1)
N(2)–Ru–N(5)	<i>b</i>	87.38(7)	87.0(1)
N(2)–Ru–N(6)	<i>b</i>	97.59(7)	97.6(1)
N(3)–Ru–N(4)	<i>b</i>	93.60(7)	93.7(2)
N(3)–Ru–N(5)	<i>b</i>	177.00(7)	176.1(1)
N(3)–Ru–N(6)	<i>b</i>	86.80(7)	90.0(1)
N(4)–Ru–N(5)	<i>b</i>	89.18(7)	86.7(1)
N(4)–Ru–N(6)	<i>b</i>	87.96(7)	85.6(1)
N(5)–Ru–N(6)	<i>b</i>	92.16(7)	86.1(2)
Ru–N(3)–O(1)	<i>b</i>	119.9(1)	174.5(3)
Ru–N(3)–O(2)	<i>b</i>	121.8(1)	<i>b</i>
O(1)–N(3)–O(2)	119.8(2)	118.3(2)	<i>b</i>
Ru–N(4)–C(11)	<i>b</i>	174.9(2)	<i>b</i>
Ru–N(5)–C(13)	<i>b</i>	176.1(2)	<i>b</i>
Ru–N(6)–C(15)	<i>b</i>	172.1(2)	<i>b</i>

^a Estimated standard deviation in the least significant figure are given in parentheses. ^b Not applicable. ^c Cent is the centroid of the *p*-cymene ring.

**Figure 1.** Labeled molecular structure of [(*p*-cym)Ru(bpy)(NO₂)]⁺ (20% ellipsoids).

cis to the nitro group only decreased in intensity by 5%. After 20 h, the acetonitrile trans to the nitro group had completely exchanged with solvent, and only 40% of the *cis* acetonitriles had exchanged.

Preparation of [Ru(bpy)(L₃)NO₂]^{0/+} and [Ru(bpy)(L₃)NO₂]^{2+/3+} Complexes. Scheme 2 shows the reactions between [Ru(bpy)(CH₃CN)₃NO₂]⁺ and Tp⁻, Tpm, and trpy to give the [Ru(bpy)(L₃)NO₂]^{0/+} complexes. All three reactions were

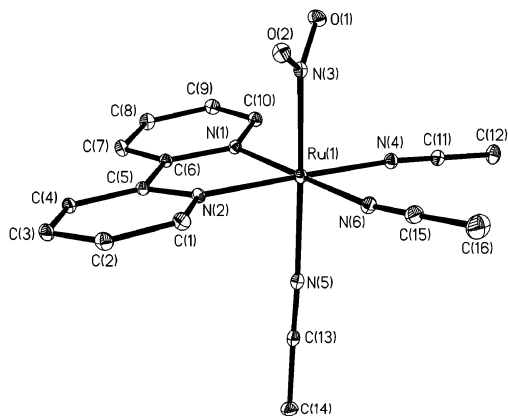


Figure 2. Labeled molecular structure of $[\text{Ru}(\text{bpy})(\text{CH}_3\text{CN})_3(\text{NO}_2)]^+$ (20% ellipsoids).

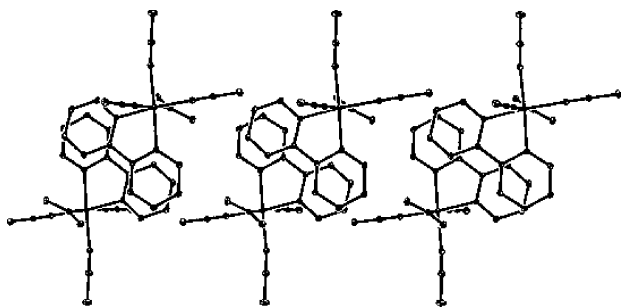


Figure 3. Solid-state packing diagram of $[\text{Ru}(\text{bpy})(\text{CH}_3\text{CN})_3(\text{NO}_2)]\text{PF}_6$. View is down the *b*-axis. Hexafluorophosphate anions are omitted for clarity.

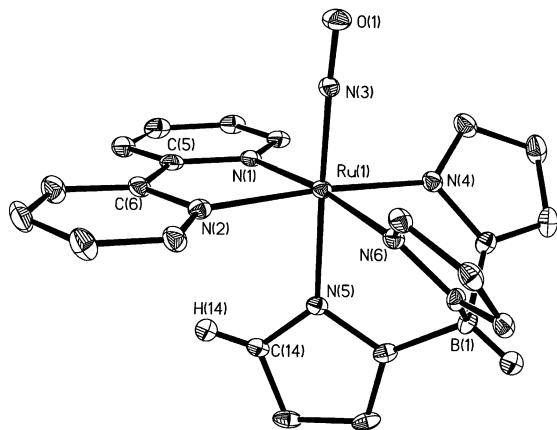
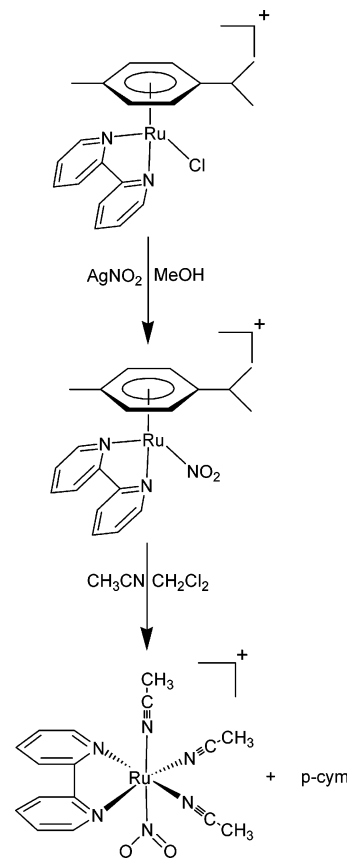


Figure 4. Labeled molecular structure of $[\text{Ru}(\text{bpy})(\text{Tp})\text{NO}]^{2+}$ (20% ellipsoids).

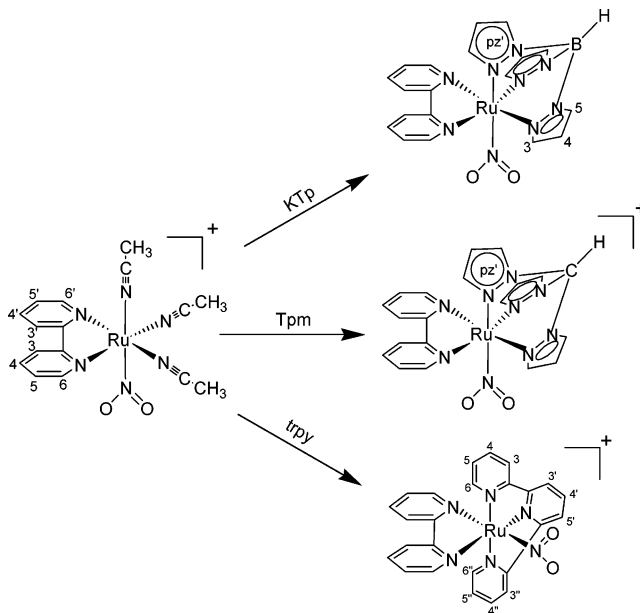
complete within 2 h, and analytically pure samples were obtained in good yield with a single recrystallization. The new $\text{Ru}(\text{bpy})(\text{Tp})\text{NO}_2$ and $[\text{Ru}(\text{bpy})(\text{Tpm})\text{NO}_2]\text{PF}_6$ complexes were isolated as maroon and orange microcrystalline solids, respectively, and were characterized by ^1H and ^{15}N NMR, IR, and UV–vis spectroscopy, cyclic voltammetry, and elemental analysis. The ^{15}N NO₂ analogues were also prepared and characterized by ^1H and ^{15}N NMR and IR spectroscopy.

The two new nitro complexes reported here react cleanly with HPF_6 to give $[\text{Ru}(\text{bpy})(\text{Tp})\text{NO}][\text{PF}_6]_2$ and $[\text{Ru}(\text{bpy})(\text{Tpm})\text{NO}][\text{PF}_6]_3$. Both complexes were also prepared with a ^{15}N -labeled nitrosyl group. $[\text{Ru}(\text{bpy})(\text{trpy})(\text{NO})][\text{PF}_6]_3$ has been prepared previously, but we also prepared that complex and the ^{15}N NO analogue. The new complexes were character-

Scheme 1



Scheme 2



ized by ^1H and ^{15}N NMR, IR, UV–vis, cyclic voltammetry, elemental analysis, and single-crystal structure determination for $[\text{Ru}(\text{bpy})(\text{Tp})\text{NO}][\text{PF}_6]_2$.

^1H NMR Studies of $[\text{Ru}(\text{bpy})(\text{L}_3)\text{NO}_2]^{0/+}$ and $[\text{Ru}(\text{bpy})(\text{L}_3)\text{NO}]^{2+/3+}$ Complexes. The ^1H NMR spectra of the Tp and Tpm compounds are complex, but a full assignment was possible using H,H-COSY. The numbering scheme for the NMR assignments is shown in Scheme 2. The ^1H NMR

Table 3. ^{15}N NMR, IR, UV–Vis, and Electrochemistry Data for Ruthenium–Nitro and Nitrosyl Compounds^a

compound	$\delta^{15}\text{N}$	ν_{NO_2}	$\nu^{15}\text{NO}_2$	ν_{NO}	$\nu^{15}\text{NO}$	UV–vis λ_{max} , nm ($\epsilon \times 10^3$, $\text{M}^{-1} \text{cm}^{-1}$)	$E_{1/2}(\text{V})^g$
$[(p\text{-cym})\text{Ru}(\text{bpy})\text{NO}_2]\text{PF}_6$	88.8	1391 1316	1354 1294	<i>d</i>	<i>d</i>	350 (sh) 316 (13) 304 (12)	
$[\text{Ru}(\text{bpy})(\text{CH}_3\text{CN})_3\text{NO}_2]\text{PF}_6$	106.8	1354 1313	1329 1289	<i>d</i>	<i>d</i>	417 (4.5) 280 (32)	
$[\text{Ru}(\text{bpy})(\text{Tp})\text{NO}_2]$	128.0 ^b	1330 ^c 1309	1307 ^c 1275	<i>d</i>	<i>d</i>	530 (sh) 471 (4.1) 303 (29)	0.617 ^h
$[\text{Ru}(\text{bpy})(\text{Tpm})\text{NO}_2]\text{PF}_6$	118.5	1340 1308	1312 1284	<i>d</i>	<i>d</i>	472 (sh) 425 (4.4) 291 (28)	1.00
$[\text{Ru}(\text{bpy})(\text{trpy})\text{NO}_2]\text{PF}_6$	118.4	1343 1302	1322 1278	<i>d</i>	<i>d</i>	472 ^f 310 291	
$[\text{Ru}(\text{bpy})(\text{Tp})\text{NO}][\text{PF}_6]_2$	−15.6	<i>d</i>	<i>d</i>	1940	1901.4	<i>e</i>	0.245 −0.631
$[\text{Ru}(\text{bpy})(\text{Tpm})\text{NO}][\text{PF}_6]_3$	−13.5	<i>d</i>	<i>d</i>	1962	1924.0	<i>e</i>	0.505 −0.473 ⁱ
$[\text{Ru}(\text{bpy})(\text{trpy})\text{NO}][\text{PF}_6]_3$	−31.6	<i>d</i>	<i>d</i>	1952	1913.0	<i>e</i>	

^a IR data were collected in a CH_3CN solution except where otherwise noted. ^{15}N NMR data were collected in a CD_3CN solution except where otherwise noted. ^b CD_2Cl_2 solution. ^c CH_2Cl_2 solution. ^d Not applicable. ^e Data not collected. ^f From ref 28. ^g Data reported for 0.5 mM solutions with 0.1 M TBAPF₆ in CH_3CN as the supporting electrolyte except where noted. Scan rates were 50 mV/s. ^h Data recorded for a 1.0 mM solution in 0.1 M TBAPF₆ in CH_2Cl_2 at a scan rate of 100 mV/s. ⁱ $E_{\text{p,c}}$, see text for detail.

spectra for the Tp and Tpm nitro and nitrosyl complexes are similar, and the following comments apply to all four complexes. Four proton signals are assigned to the bipyridine ligand, consistent with the expected C_s symmetry. The pz ring proton resonances are also consistent with this geometry. Two sets of three signals are observed in a 2:1 ratio, which are readily identified from their coupling patterns as arising from the pz rings. The more intense signals are assigned to the protons on the chemically equivalent pz rings trans to the bipyridine. The other set of pz resonances are assigned to the pz ring trans to the nitro group (designated as pz'). Additional confirmation of this assignment is provided by the unusual chemical shift of H^3 on pz'. This proton resonates at 1.5–2.0 ppm upfield of H^3 on the other two pz rings and the H^5 protons on both sets of pz rings. This can be attributed to the proximity of H^3 on pz' to the shielding portion of the anisotropic ring current on the bipyridine ring. This effect has been observed in other ruthenium–bipyridine complexes⁴⁹ and was useful here in assigning the resonances for the pz protons. In the absence of the ring current effect, the pz H^3 and H^5 protons have very similar chemical shifts and are difficult to assign. With H^3 on pz' shifted upfield, the remaining downfield pz resonance that integrates as one proton must be H^5 on pz'. With this unambiguous assignment of H^3 and H^5 on the pz' rings for all four complexes, we noted that $J_{\text{H}^4-\text{H}^5}$ is consistently greater than $J_{\text{H}^4-\text{H}^3}$, as has been previously observed in related Tp⁵⁵ and Tpm⁵⁶ complexes. The difference in the coupling constants could then be used to assign the H^3 and H^5 protons on the pz rings trans to bipyridine.

Although $[\text{Ru}(\text{bpy})(\text{trpy})\text{NO}_2]^+$ and $[\text{Ru}(\text{bpy})(\text{trpy})\text{NO}]^{3+}$ have been previously prepared,⁴⁰ no ^1H NMR data was reported. The following comments apply to both the nitro and nitrosyl complexes. There were several resonances that could not be resolved, but an essentially complete assignment could be made using 1D proton and H,H–COSY experiments. Seven signals are assigned to the trpy ligand with six integrating as two protons and one integrating as one proton. This is consistent with the complex having C_s symmetry in which a plane of symmetry bisects the trpy ligand. Eight separate signals, all integrating as a single proton, were observed for the bipyridine ligand, consistent with the nonequivalence of the two bpy rings. The chemical shifts of the protons on the two bpy ring spin systems are significantly different, with one set appearing consistently upfield of the other. The greatest difference is with the $\text{H}^{6,6'}$ protons, which exhibit a 2.6 ppm difference in chemical shift. In assigning the spectrum, we assumed that the set of bpy protons with the upfield chemical shift belongs to the bpy ring trans to the nitro group. The upfield shift is due to the proximity of the protons on that ring to the shielding portion of the trpy anisotropic ring current.

IR Studies. Table 3 gives the IR stretching frequencies for the nitro and nitrosyl complexes, including the ^{15}N -labeled complexes. The ^{15}N labeling is particularly helpful in identifying the nitro stretches because of the presence of numerous other ligand vibrations in the same region as the nitro stretches (1300–1400 cm^{-1}). The nitro group in N-bound metal–nitro complexes typically displays symmetric (ν_{sym}) and asymmetric (ν_{asym}) stretches with the asymmetric stretch having the higher frequency.⁵⁷ The IR spectra of the new nitro complexes reported here all exhibit

(55) Jalon, F. A.; Otero, A.; Rodriguez, A. *J. Chem. Soc., Dalton Trans.* **1995**, 1629.

(56) Katz, N. E.; Romero, I.; Llobet, A.; Parella, T.; Benet-Buchholz, J. *Eur. J. Inorg. Chem.* **2005**, 272.

(57) Cotton, F. A.; Wilkinson, G. *Advanced Inorganic Chemistry*, 5th ed.; Wiley & Sons: New York, 1988; p 486.

two peaks between 1300 and 1400 cm^{-1} that shift 20 – 40 cm^{-1} to lower frequency in the $^{15}\text{NO}_2$ -labeled complexes. On the basis of this, we assign the peaks to the ν_{sym} and ν_{asym} stretching modes. The ν_{asym} peaks are between 1320 and 1391 cm^{-1} , and the ν_{sym} peaks range from 1302 to 1315 cm^{-1} . The ν_{asym} value for $[(p\text{-cym})\text{Ru}(\text{bpy})\text{NO}_2]^+$ is unusually high (1391 cm^{-1}) for a ruthenium–nitro complex. The closest compound for comparison we could find is $[\text{Ru}_2(6,6'\text{-Me}_2\text{dppz})(\eta^6\text{-}p\text{-cymene})_2\text{Cl}_2]\text{PF}_6$ ($6,6'\text{-Me}_2\text{dppz} = 2,2'-(1H\text{-pyrazole-}3,5\text{-diyl})\text{bis}(6\text{-methylpyridine})$) in which the nitro ν_{asym} is 1367 cm^{-1} .⁵⁸ The nitro stretching frequencies for the other compounds lie within the ranges expected from comparison to literature data for other ruthenium–nitro compounds.^{30,47} The observed isotopic shift is also consistent with previous studies.^{31,35,59}

The IR spectra of $[\text{Ru}(\text{bpy})(\text{Tp})\text{NO}][\text{PF}_6]_2$ and $[\text{Ru}(\text{bpy})(\text{Tpm})\text{NO}][\text{PF}_6]_3$ show intense bands at 1940 and 1962 cm^{-1} , respectively, that are assigned to ν_{NO} of the nitrosyl ligand. Both values are close to those reported for other Ru(II) complexes with similar ligand systems; however, $[\text{Ru}(\text{bpy})(\text{Tpm})\text{NO}]^{3+}$ has, by a small margin, the highest nitrosyl stretching frequency reported for a Ru(II)–nitrosyl complex.¹² The nitrosyl bands shift 40 cm^{-1} to lower frequency in the ^{15}NO -labeled complexes. The experimental $\nu^{14}\text{NO}/\nu^{15}\text{NO}$ ratios are 1.021 , 1.020 , and 1.020 for the Tp, Tpm, and trpy complexes, respectively, very close to the theoretical value of 1.018 calculated with the Hooke's Law approximation.

^{15}N NMR Studies. ^{15}N NMR spectra for these complexes are easily obtained on the 100% labeled complexes. The ^{15}N chemical shifts referenced to neat CD_3NO_2 are given in Table 3. The $^{15}\text{NO}_2$ signals range from 89 ppm for $[(p\text{-cym})\text{Ru}(\text{bpy})\text{NO}_2]\text{PF}_6$ to 128 ppm for $[\text{Ru}(\text{bpy})\text{TpNO}_2]$. These values are consistent with those generally observed for metal–nitro complexes⁶⁰ and the few ruthenium–nitro complexes for which data are available.^{18,31,61} The ^{15}N chemical shifts of the nitrosyl groups in the $[\text{Ru}(\text{bpy})(\text{L}_3)\text{NO}]^{2+/3+}$ complexes are at the low end of the chemical shift range observed for linear metal–nitrosyl complexes but are typical for $\{\text{Ru}-\text{NO}\}^6$ complexes.^{60,62}

UV–Vis Spectroscopy. UV–vis data for the four new nitro complexes are shown in Figure 5, and the data are summarized in Table 3. All four complexes have similar spectra, displaying intense bands ($\epsilon > 20\,000\text{ cm}^{-1}\text{ M}^{-1}$) below 350 nm and less intense ($\epsilon < 5000\text{ cm}^{-1}\text{ M}^{-1}$) broader bands at longer wavelengths. For $[(p\text{-cym})\text{Ru}(\text{bpy})\text{NO}_2]\text{PF}_6$, the longer wavelength band is not resolved, appearing as a shoulder on the more intense UV peaks. By comparison with related complexes, the higher energy bands can be assigned to a ligand-centered transition; the weaker visible bands are most likely $\pi^*(\text{bpy}) \leftarrow d\pi(\text{Ru})$ MLCT transitions.^{27,56,63,64}

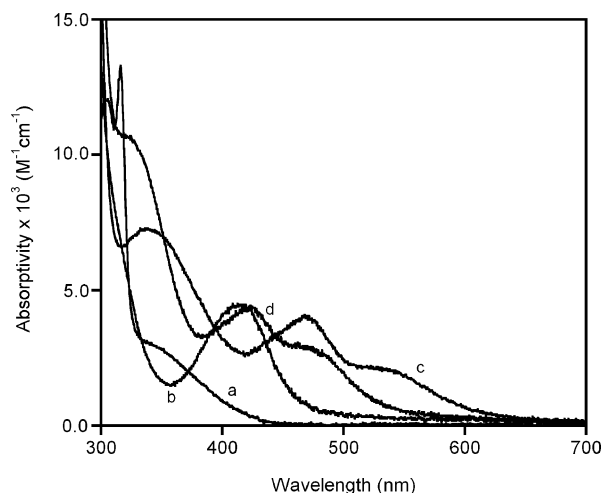


Figure 5. UV–vis spectra of $[(p\text{-cym})\text{Ru}(\text{bpy})\text{NO}_2]\text{PF}_6$ (a, CH_2Cl_2 solution), $[\text{Ru}(\text{bpy})(\text{CH}_3\text{CN})_3\text{NO}_2]\text{PF}_6$ (b, CH_3CN solution), $[\text{Ru}(\text{bpy})(\text{Tp})\text{NO}_2]$ (c, CH_3CN solution), $[\text{Ru}(\text{bpy})(\text{Tpm})\text{NO}_2]\text{PF}_6$ (d, CH_3CN solution).

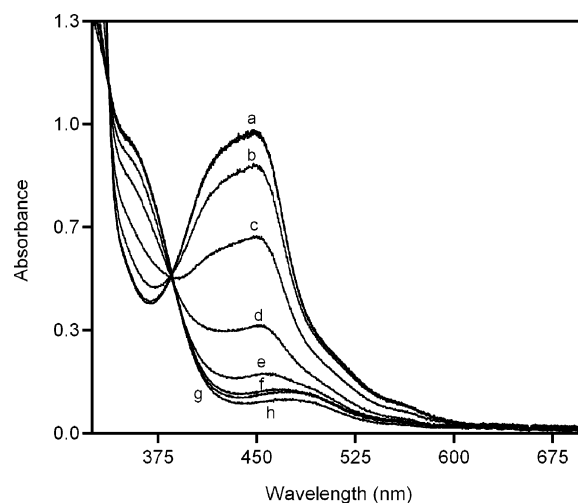


Figure 6. UV–vis spectra of $[\text{Ru}(\text{bpy})(\text{trpy})\text{NO}_2]\text{Cl}$ at different pH's after 2 days: a = 4.8 and 5.3, b = 3.8, c = 3.5, d = 3.2, e = 2.9, f = 2.6, g = 2.3, h = 2.0.

Equilibrium Studies. The equilibrium constant for reaction 2 was determined for $\text{L}_3 = \text{Tpm}$ and trpy. $[\text{Ru}(\text{bpy})(\text{Tp})\text{NO}_2]$ was not sufficiently soluble in water to be studied. Figure 6 shows the UV–vis spectrum of $[\text{Ru}(\text{bpy})(\text{trpy})\text{NO}_2]^+$ at different pH's after equilibrating at $25.0 (\pm 0.1)^\circ\text{C}$ for 2 days. Isosbestic points are observed at 337 and 386 nm , consistent with the presence of only the two absorbing species shown in reaction 2. A Scatchard plot derived from these data is shown in Figure 7. From eq 3, the slope of this plot equals $-K_{\text{eq}}$, giving $K_{\text{eq}} = 1.70(7) \times 10^{21}\text{ M}^{-2}$. This equilibrium constant was previously reported to be $2.1 \times 10^{23}\text{ M}^{-2}$, but no experimental details were provided,^{27,43} and so we are unable to account for the difference. Similar data were obtained for the equilibrium between $[\text{Ru}(\text{bpy})(\text{Tpm})\text{NO}]^{3+}$ and $[\text{Ru}(\text{bpy})(\text{Tpm})\text{NO}_2]^+$ (Figures S1 and S2) and K_{eq} was determined to be $2.5(3) \times 10^{22}\text{ M}^{-2}$.

(58) Catalano, V. J.; Craig, T. J. *Polyhedron* **2000**, *19*, 475.

(59) Leising, R. A.; Kubow, S. A.; Churchill, M. R.; Buttrey, L. A.; Ziller, J. W.; Takeuchi, K. J. *Inorg. Chem.* **1990**, *29*, 1306.

(60) Mason, J.; Larkworthy, L. F.; Moore, E. A. *Chem. Rev.* **2002**, *102*, 913.

(61) Emel'yanov, V.; Fedotov, M.; Belyaev, A. Z. *Neoorg. Khim.* **1993**, *38*, 1842.

(62) Bell, L. K.; Mason, J.; Mingos, D. M. P.; Tew, D. G. *Inorg. Chem.* **1983**, *22*, 3497.

(63) Katz, N. E.; Fagalde, F.; Katz, N. D. L.; Mellace, M. G.; Romero, I.; Llobet, A.; Benet-Buchholz, J. *Eur. J. Inorg. Chem.* **2005**, 3019.

(64) Huang, L.; Seward, K. J.; Sullivan, B. P.; Jones, W. E.; Mecholsky, J. J.; Dressick, W. J. *Inorg. Chim. Acta.* **2000**, *310*, 227.

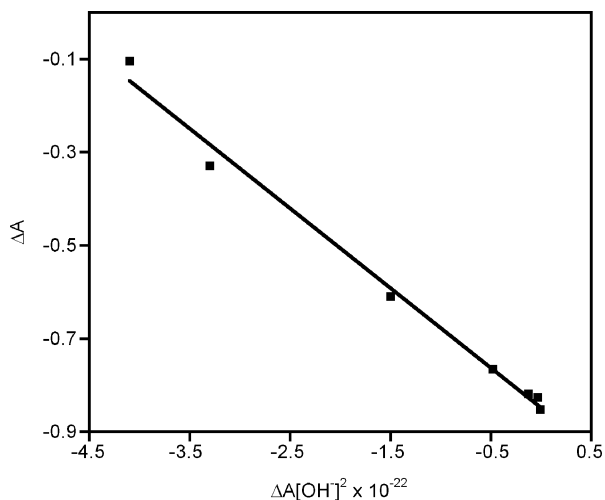


Figure 7. Scatchard plot for pH-dependent equilibrium between $[\text{Ru}(\text{bpy})\text{-(trpy)NO}_2]^+$ and $[\text{Ru}(\text{bpy})(\text{trpy})\text{NO}]^{3+}$. Absorbance values were measured at 450 nm. Fitting parameters: slope = $(-1.70 \pm 0.07) \times 10^{21} \text{ M}^{-2}$, intercept = -0.849 ± 0.01 .

Electrochemical Studies. Electrochemical data for $[\text{Ru}(\text{bpy})(\text{Tp})\text{NO}_2]$, $[\text{Ru}(\text{bpy})(\text{Tpm})\text{NO}_2]^+$, $[\text{Ru}(\text{bpy})(\text{Tpm})\text{NO}]^{3+}$, and $[\text{Ru}(\text{bpy})(\text{Tp})\text{NO}]^{3+}$ are given in Table 3. Cyclic voltammograms for $[\text{Ru}(\text{bpy})(\text{Tp})\text{NO}_2]$ and $[\text{Ru}(\text{bpy})(\text{Tp})\text{NO}]^{2+}$ are shown in Figures S3 and S4, respectively. Both nitro complexes can be oxidized, with the Tp complex oxidizing at a potential almost 0.4 V less than the Tpm complex. The oxidation of the Tp complex is reversible; in contrast, the oxidation of the Tpm complex is only partially reversible at a scan rate of 50 mV/s ($i_{p,c}/i_{p,a} = 0.7$). Comparison to other ruthenium–nitro complexes indicates that these waves correspond to the oxidation of Ru(II) to Ru(III).^{1,4,12,34,44} The nitrosyl complexes both display two widely separated reduction waves. The first process is reversible for both complexes; the more negative wave is reversible for the Tp complex and irreversible for the Tpm complex. On the basis of detailed studies of similar complexes, it is likely that both reductions are one-electron processes centered at the nitrosyl ligand.^{1,4,6,10,12,28} The first wave represents the formal reduction of the nitrosyl ligand from NO^+ to NO^\bullet , and the second wave represents further reduction to NO^- . The more positive reduction potentials of the Tpm vs the Tp complex support this assignment.

X-ray Studies. The ORTEP of $[(p\text{-cym})\text{Ru}(\text{bpy})\text{NO}_2]^+$ (Figure 1) shows a symmetrically coordinated *p*-cymene ligand with a ring-centroid to ruthenium distance of 1.710 Å, similar to the analogous values (1.717 and 1.731 Å) observed for $[(p\text{-cym})\text{RuNO}_2]_2\text{H}_2(6,6'\text{-Me}_2\text{dppz})$ ($6,6'\text{-Me}_2\text{-dppz} = 2,2'\text{-(pyrazole-3,5-diyl)bis(6-methylpyridine)}$), the only other example of a ruthenium–arene complex with a nitro ligand we could find in the literature.⁵⁸ The nitro group is N-bound, consistent with the IR data. The O–N–O angle in the nitro group is $119.8(2)^\circ$, within the $113\text{--}127^\circ$ range generally observed for M–NO_2 complexes.⁴⁷

The ORTEP of the $[\text{Ru}(\text{bpy})(\text{CH}_3\text{CN})_3\text{NO}_2]^+$ cation (Figure 2) shows the ruthenium is essentially octahedrally coordinated with the exception of the bpy bite angle of $79.35\text{--}(7)^\circ$. The angles between the three acetonitrile ligands and

the nitro group range $86.80(7)\text{--}93.60(7)^\circ$. The structure confirms the assignment of *fac* geometry suggested by the NMR data and confirms that the nitro group is N-bound, as indicated by the IR spectrum. The O–N–O angle in the nitro group is 118.25° , similar to the value observed for $[(p\text{-cym})\text{Ru}(\text{bpy})\text{NO}_2]\text{PF}_6$. The three acetonitrile ligands are coordinated in an essentially linear fashion with the Ru–N–CCH₃ angles ranging $172.1(2)\text{--}176.1(2)^\circ$. The Ru–NCCH₃ bond lengths are essentially equivalent for the acetonitrile ligands trans to bipyridine at 2.046(2) and 2.045(2) Å. The Ru–NCCH₃ bond to the acetonitrile trans to the nitro group is significantly longer at 2.076(2) Å. The packing of the cations (Figure 3) in the structure of $[\text{Ru}(\text{bpy})(\text{CH}_3\text{CN})_3\text{NO}]\text{PF}_6$ is interesting. The cations pack as pairs with the nitro groups oriented anti to each other with π -stacking interactions between the bipyridine ligands. The bipyridine ligands are parallel with a 0° angle between the bpy least-squares planes. The π -stacking distance is 3.42 Å, similar to the 3.4 Å van der Waals (vdw) thickness of the bipyridine π -system.⁶⁵

The ORTEP of the $[\text{Ru}(\text{bpy})(\text{Tp})\text{NO}]^{2+}$ cation (Figure 4) shows essentially octahedral coordination about the Ru and confirms that the Tp ligand occupies a trigonal face of the complex. The bpy bite angle is $78.7(2)^\circ$, but the bond angles between the three coordinated nitrogens of the Tp ligand and the nitrogen of the NO group are between $85.6(1)^\circ$ and $93.7\text{--}(2)^\circ$, giving the complex essentially octahedral geometry. The NO ligand is close to linearly coordinated with a Ru–N–O bond angle of $174.5(3)^\circ$, consistent with the IR and ¹⁵N NMR data. The distance between the hydrogen on C(14) and the centroid of the C(5)–C(6) bond on the bipyridine ligand is 2.84 Å, consistent with the conjecture that the unusual upfield shift observed for this proton in the ¹H NMR spectrum is due to its proximity to the shielding portion of the anisotropic ring current of the bipyridine ligand.⁶⁶

Discussion

The synthesis of $[\text{Ru}(\text{bpy})(\text{CH}_3\text{CN})_3\text{NO}_2]\text{PF}_6$ is accomplished in four simple, high yield steps starting from RuCl_3 . The first two steps, the preparations of $[(p\text{-cym})\text{RuCl}_2]_2$ and $[(p\text{-cym})\text{Ru}(\text{bpy})\text{Cl}]\text{PF}_6$, are simple literature procedures. The preparation of $[(p\text{-cym})\text{Ru}(\text{bpy})\text{NO}_2]\text{PF}_6$ required that Ag^+ be used to assist in removing the chloride from $[(p\text{-cym})\text{Ru}(\text{bpy})\text{Cl}]^+$. In the absence of Ag^+ , either no reaction is observed (room temperature) or $[\text{Ru}(\text{bpy})(\text{NO}_2)_4]^{2-}$ is obtained (reflux). By using Ag^+ , the nitro group can also be added with only a slight excess of nitrite ion, making it economical to prepare the ¹⁵NO₂ analogue. This is in contrast with the typical literature preparations of Ru–NO₂ complexes in which a 10–20-fold excess of NO₂[−] is required. The final step, the preparation of $[\text{Ru}(\text{bpy})(\text{CH}_3\text{CN})_3\text{NO}_2]^+$, requires strict attention to detail. If $[(p\text{-cym})\text{Ru}(\text{bpy})\text{NO}_2]^+$ is refluxed in neat acetonitrile, conversion to $[\text{Ru}(\text{bpy})(\text{CH}_3\text{CN})_3\text{NO}_2]^+$ is followed by decomposition to unknown products to give

(65) The vdw thickness of bpy is assumed to be twice the vdw radius of C given in: Bondi, A. *J. Phys. Chem.* **1964**, *68*, 441.

(66) Schneider, H.; Rudiger, V.; Cuber, U. *J. Org. Chem.* **1995**, *60*, 996.

an intractable mixture. We found that using a 2:1 mixture of methylene chloride and acetonitrile still gives complete conversion to $[\text{Ru}(\text{bpy})(\text{CH}_3\text{CN})_3\text{NO}_2]^+$ in a reasonable time (20 h) and provides analytically pure product directly from the reaction.

The displacement of *p*-cymene by acetonitrile under such mild conditions is rather surprising. Although thermal arene displacement reactions from ruthenium are known, they are rare and generally require either more forcing conditions or better nucleophiles than acetonitrile.^{67–73} The nitro group clearly plays a roll in labilizing the *p*-cymene ring. When the reaction of $[(p\text{-cym})\text{Ru}(\text{bpy})\text{NO}_2]^+$ at 40 °C in CD_3CN was followed by ^1H NMR spectroscopy, approximately 100% conversion to $[\text{Ru}(\text{bpy})(\text{CD}_3\text{CN})_3\text{NO}_2]^+$ occurred within about 24 h. Under the same conditions, $[(p\text{-cym})\text{Ru}(\text{bpy})\text{-Cl}]^+$ showed no observable reaction in 2 weeks. One possible explanation for this difference is suggested by the reactivity of $[\text{Ru}(\text{bpy})(\text{CH}_3\text{CN})_3\text{NO}_2]^+$ in CD_3CN solution, which indicates that the nitro has a trans-labilizing effect. The acetonitrile trans to the nitro group exchanges with solvent at a rate approximately 20 times as fast as the acetonitriles cis to the nitro. The crystal structure of $[\text{Ru}(\text{bpy})(\text{CH}_3\text{-CN})_3\text{NO}_2]^+$ indicates that the trans effect might be partially due to a ground state trans influence as the $\text{Ru}-\text{NCCH}_{3\text{trans}}$ bond is 0.030(4) Å longer than the $\text{Ru}-\text{NCCH}_{3\text{cis}}$ bonds. Presumably, the nitro group could also exert a trans-influence on the *p*-cymene ring in $[(p\text{-cym})\text{Ru}(\text{bpy})\text{NO}_2]^+$, which would make it more susceptible to substitution. We are engaged in kinetic and structural studies to further address this issue.

Reaction of $[\text{Ru}(\text{bpy})(\text{CH}_3\text{CN})_3\text{NO}_2]^+$ in acetone with tridentate ligands gives rapid, clean conversion to $[\text{Ru}(\text{bpy})\text{-}(\text{L}_3)\text{NO}_2]$ complexes. The reactions with Tp and Tpm are somewhat sensitive to reaction time, resulting in decomposition if the reaction is allowed to go much longer than 2 h. In comparison, the reaction with trpy gives an initial product of higher purity, and the reaction is less sensitive to reaction time. The facial geometry of $[\text{Ru}(\text{bpy})(\text{CH}_3\text{CN})_3\text{NO}_2]^+$ suggests that reactions with fac-coordinating ligands such as Tp and Tpm would be less complex. However, it appears that the nitro group can readily isomerize from the position trans to acetonitrile to trans to bipyridine when $[\text{Ru}(\text{bpy})\text{-}(\text{CH}_3\text{CN})_3\text{NO}_2]^+$ reacts with a ligand that prefers to form a complex with mer geometry.

The overall synthetic strategy described here is a useful alternative to standard preparations of ruthenium–nitro complexes. Typical synthetic routes use halide complexes ($[\text{Ru}(\text{trpy})\text{Cl}_3]$ and $[\text{Ru}(\text{bpy})_2\text{Cl}_2]$, for example), and presum-

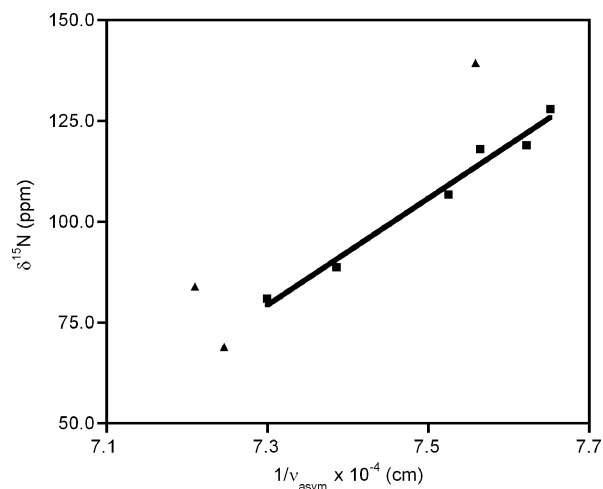


Figure 8. Plot of ^{15}N chemical shift versus ν_{asym} for the nitro group for the complexes given in Table 3: (■) complexes with one nitro group; (▲) complexes with two nitro groups. The best-fit line does not include complexes with two nitro groups. Fitting parameters: slope = $(1.3 \pm 0.1) \times 10^6$ ppm/cm, intercept = $-8.9 \pm 0.8 \times 10^2$ ppm.

ably, similar precursors containing the Tp and Tpm ligands could be prepared. However, adding these ligands to a common synthon has a clear advantage, especially when it is considered that a variety of nitro complexes can now be prepared with systematic variations in electronic and steric properties using available ligands. A second advantage of this synthetic route is the stoichiometric introduction of the nitro group, making it very economical to prepare ^{15}N -labeled nitro and nitrosyl compounds. Because of the presence of many ligand-centered vibrational modes in the 1300–1400 cm^{-1} region, the ^{15}N labeling is clearly useful in identifying the nitro stretching bands in the IR spectra of these complexes. In addition, it becomes possible to easily collect ^{15}N NMR data, a useful but under-utilized technique for characterizing ruthenium–nitro and –nitrosyl complexes. With 100% ^{15}N labeling, it is possible to collect a ^{15}N NMR spectrum in less than 30 min on a 7 T instrument at 10 mM concentrations.

The ^{15}N NMR data reported here demonstrate the potential of this technique when applied to a significant number of ruthenium–nitro complexes. The chemical shifts occur over about 30 ppm, a relatively small chemical shift range for a heteroatom, but it is interesting to note that the data in Table 3 do show a strong correlation between the ^{15}N NMR chemical shifts, the nitro stretching frequencies, and the MLCT transition energies. As the ^{15}N chemical shift decreases, the asymmetric stretching frequency of the nitro group and the MLCT transition energy increase. To explore this further, the ^{15}N chemical shift was plotted against the reciprocal of the nitro asymmetric stretching frequency (ν_{asym}), as shown in Figure 8. Included are data for the nitro complexes reported here as well as the following compounds from the literature for which suitable IR and ^{15}N NMR data are available: $\text{K}_2[\text{Ru}(\text{bpy})(\text{NO}_2)_4]^{31}$ ($\delta^{15}\text{N} = 138, 141$ ppm; $\nu_{\text{asym}} = 1327, 1318$ cm^{-1}), *cis,trans*- $\text{Ru}(\text{bpy})(\text{NO}_2)_2(\text{NO})(\text{OH})^{31}$ ($\delta^{15}\text{N} = 84$ ppm; $\nu_{\text{asym}} = 1387$ cm^{-1}), *cis,cis*- $\text{Ru}(\text{bpy})(\text{NO}_2)_2(\text{ONO})(\text{NO})^{31}$ ($\delta^{15}\text{N} = 70, 68$ ppm; $\nu_{\text{asym}} = 1387, 1373$ cm^{-1}), $\text{Ru}(\text{hedta})(\text{NO})(\text{NO}_2)^{18}$ ($\delta^{15}\text{N} = 81$ ppm; $\nu_{\text{asym}} = 1370$

(67) Major, Q.; Lough, A. J.; Gusev, D. G. *Organometallics* **2005**, *24*, 2492.

(68) Tai, C.; Pitts, J.; Linchen, J. C.; Main, A. D.; Munchi, P.; Jessop, P. G. *Inorg. Chem.* **2002**, *41*, 1606.

(69) Widegren, J. A.; Bennett, M. A.; Finke, R. G. *J. Am. Chem. Soc.* **2003**, *125*, 10301.

(70) Tobita, H.; Hosegawa, K.; Minglana, J. J. G.; Luh, L.; Okazaki, M.; Ogino, H. *Organometallics* **1999**, *18*, 2058.

(71) Green, M. L. H.; Joyner, D. S.; Wallis, J. M. *J. Chem. Soc., Dalton Trans.* **1987**, 2823.

(72) Bennett, M. A.; Matheson, T. W.; Roberson, G. B.; Smith, A. K.; Tucker, P. A. *Inorg. Chem.* **1980**, *19*, 1014.

(73) Bennett, M. A.; Smith, A. K. *J. Chem. Soc., Dalton Trans.* **1974**, 233.

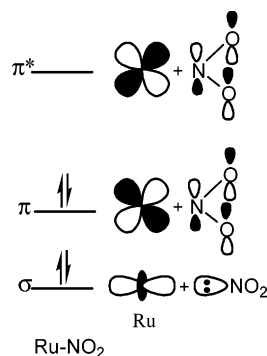


Figure 9. Qualitative molecular orbital diagram for a ruthenium–nitro complex showing σ -bonding (σ), π -bonding (π), and π -antibonding (π^*) levels.

cm^{-1} ; $\text{hedta}^{3-} = N$ -(hydroxyethyl)ethylenediaminetriacetate).⁷⁴ A reasonable correlation between $\delta^{15}\text{N}$ and $1/\nu_{\text{asym}}$ is present for all of complexes, but a good linear relationship is observed if only the compounds with a single nitro ligand are considered. We plan to explore this relationship in more detail, but it seems likely that it stems from the dependence of the ^{15}N chemical shift on charge circulation caused by magnetic field induced mixing of the σ and π^* orbitals shown in the simplified MO diagram of a ruthenium–nitro complex in Figure 9. Theoretical work^{60,75} indicates that the ^{15}N nucleus should be deshielded as the difference in energy (ΔE) between the σ and π^* orbitals decreases. A net increase in the electron density at the metal caused by an electron donating ligand would raise the energy of both the σ and π orbitals in Figure 9. This would result in a great ^{15}N chemical shift (smaller ΔE resulting in greater deshielding) and a lower nitro stretching frequency due to increased back-bonding from the filled $d\pi$ orbitals of the ruthenium to the π^* orbitals

(74) The ^{15}N chemical shifts for these compounds were reported relative to formamide and were converted to the CH_3NO_2 scale.

(75) Penner, G. H.; Bernard, G. M.; Wasylishen, R. E.; Barrett, A.; Curtis, R. D. *J. Org. Chem.* **2003**, *68*, 4258.

of the nitro group. Overall, this leads to the correlation observed in Figure 8. Detailed modeling studies of these complexes would certainly be needed to support this hypothesis. From a practical point of view, the high quality of the correlation in Figure 8 suggests that the ^{15}N NMR chemical shifts, like IR and UV–vis data, provide information about the electron density at the metal center.

Conclusions

We have successfully prepared a ruthenium–nitro synthon that readily exchanges three acetonitrile ligands for mer- or fac-coordinating tridentate ligands. Using this synthon, we have prepared two new ruthenium–nitro complexes, $[\text{Ru}(\text{bpy})(\text{Tp})\text{NO}_2]$ and $[\text{Ru}(\text{bpy})(\text{Tpm})\text{NO}_2]^+$ and their nitrosyl analogues. This synthetic route also allows for the simple and economical introduction of a ^{15}N label on the nitro and nitrosyl groups which simplifies both the assignment of IR spectra and the acquisition of ^{15}N NMR data. We will continue to expand on this synthetic methodology by substituting different bidentate ligands for bipyridine to give other $[\text{Ru}(\text{L}_2)(\text{CH}_3\text{CN})_3\text{NO}_2]$ complexes from which “families” of $[\text{Ru}(\text{L}_2)(\text{L}_3)\text{NO}_2]$ complexes can be prepared.

Acknowledgment. We gratefully acknowledge the help of Dr. Joe Tanski of Vassar College with the single crystal X-ray studies and the NSF (grant no. 0521237) for funding the Vassar College X-ray crystallography facility. We also acknowledge the financial support of The State University of New York at New Paltz.

Supporting Information Available: Text file of crystal data. UV–vis spectra and Scatchard plot for the determination of the equilibrium between $[\text{Ru}(\text{bpy})(\text{Tpm})\text{NO}]^{3+}$ and $[\text{Ru}(\text{bpy})(\text{Tpm})\text{NO}_2]^+$ and cyclic voltammograms of $[\text{Ru}(\text{bpy})(\text{Tp})\text{NO}_2]$ and $[\text{Ru}(\text{bpy})(\text{Tp})\text{NO}]^{2+}$. This material is available free of charge via the Internet at <http://pubs.acs.org>.

IC061039T